Available online at www.sciencedirect.com
SCIENCE DIRECT®
Journal of Magnetic Resonance 169 (2004) 323–327
JMR Journal of Magnetic Resonance
www.elsevier.com/locate/jmr

A distributed equivalent magnetic current based FDTD method for the calculation of E-fields induced by gradient coils

Feng Liu and Stuart Crozier*

The School of Information Technology and Electrical Engineering, The University of Queensland, St. Lucia, Brisbane, Queensland 4072, Australia

Received 24 March 2004; revised 12 May 2004
Available online 5 June 2004

Abstract

This paper evaluates a new, low-frequency finite-difference time-domain method applied to the problem of induced E-fields/eddy currents in the human body resulting from the pulsed magnetic field gradients in MRI. In this algorithm, a distributed equivalent magnetic current is proposed as the electromagnetic source and is obtained by quasistatic calculation of the empty coil's vector potential or measurements therein. This technique circumvents the discretization of complicated gradient coil geometries into a mesh of Yee cells, and thereby enables any type of gradient coil modelling or other complex low frequency sources. The proposed method has been verified against an example with an analytical solution. Results are presented showing the spatial distribution of gradient-induced electric fields in a multi-layered spherical phantom model and a complete body model.

Keywords: FDTD; Low frequency electromagnetic wave; Total/scattered Field; Eddy current; Gradient coil; Human model

1. Introduction

Numerical modelling of the E-fields or eddy currents induced in the human body by the pulsed field gradients in MRI presents a difficult computational problem. It requires an efficient and accurate computational method for high spatial resolution analyses with a relatively low input frequency by computational electromagnetic standards. Several methods, including analytic [1,2], finite element [3], impedance [4], and finite-difference [5,6] have been developed for the evaluation of the eddy currents in biologically relevant samples. Among them, the finite-difference time-domain (FDTD) method [7–11] has been used extensively for MRI applications. Some of the technical problems that first appeared in relation to the application of FDTD scheme to low frequency problems such as gradient switching have been solved to some extent. For example, in order to circumvent the unacceptable computation time required to use conventional FDTD technique at low frequencies, an effective Fourier analysis-based time/frequency numerical conversion technique [10] and a quasistatic approximation approach [9] by alternating the transmission media (setting the relative permittivity to unity) have been proposed to improve the convergence speed. As source injection in the FDTD simulation plays a crucial rule in obtaining accurate solutions, a voltage source model [11] has been constructed by making use of the derivative of the input source waveform and advantages over direct current source injection demonstrated.

In low-frequency, current-source based FDTD algorithms [10,11], gradient coils are modelled as standard current/voltage sources and discretized into a mesh of Yee cells; however, when the coil geometry becomes complex, this becomes both difficult and inaccurate. The use of distributed source fields has previously been used [7–9] to assist with this problem.

In this report, a modified, distributed equivalent magnetic currents (DEMC) based FDTD method is proposed to further enable complex, low frequency source modelling. It has been demonstrated that the total-field/scattered-field concept can be used to for-

* Corresponding author. Fax +61-7-3365-4999.
E-mail address: stuart@itee.uq.edu.au (S. Crozier).

1090-7807/$ - see front matter © 2004 Elsevier Inc. All rights reserved.
doi:10.1016/j.jmr.2004.05.011

mulate a low-frequency FDTD algorithm, where the electromagnetic source can be simply obtained by quasistatic calculation of the empty coil's vector potential or measurements therein. This source model successfully circumvents the discretization procedure of complicated coil geometries, and therefore can be used to investigate a variety of gradient sets in MRI.

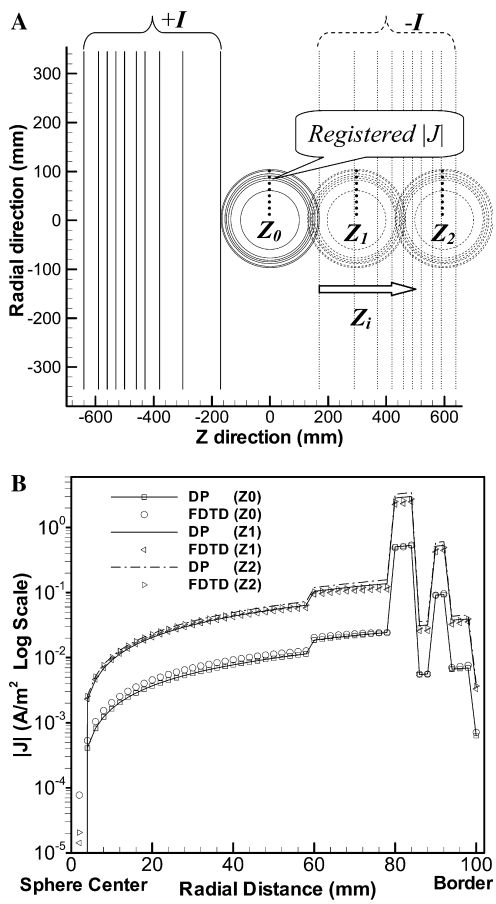

Fig. 1. Calculation of the eddy currents ($|J|$) inside the seven-layered spherical phantom excited by a typical z–gradient coil system [14]. (A) Schematic arrangement of the phantom inside the coils. To generate a slew rate of $dB/dz/dt \approx T/m/s$, the coil current is about $\boldsymbol{I} = \pm 500.0\ A$ and the frequency is 1 kHz. The induced fields were calculated as a function of phantom position with respect to the gradient system. (B) Comparisons of Debye Potential (DP) based analytic solution [18] and FDTD solution along the radial distance at $y = 0$. The field values are shown for three different positions: $z = 0$, 0.3, and 0.6 m (Z_0, Z_1, Z_2), respectively.

2. Theory

Due to the linearity of Maxwell's equations [12], the electric and magnetic fields can be expressed as the summation of the incident components and scattered components, i.e., $\mathbf{E} = \mathbf{E}_i + \mathbf{E}_s, \mathbf{H} = \mathbf{H}_i + \mathbf{H}_s$. $\mathbf{E}_i, \mathbf{H}_i$ are the values of the incident wave fields, which are easily obtained at all space points of the FDTD grid. $\mathbf{E}_s, \mathbf{H}_s$ are the unknowns of the scattered wave fields, which are resultant from the interaction of the gradient fields with the human body.

If Faraday's law is written as

$$\nabla \times \mathbf{E} = -\mu\partial(\mathbf{H}_i + \mathbf{H}_s)/\partial t. \tag{1}$$

Then

$$\mu\partial\mathbf{H}_s/\partial t = -\nabla \times \mathbf{E} - \mu\partial\mathbf{H}_i/\partial t = -\nabla \times \mathbf{E} + \mathbf{M}_i, \tag{2}$$

Where $\mathbf{M}_i$ is the defined distributed equivalent magnetic current (DEMC) with can be expressed as

$$\mathbf{M}_i = -\mu\partial\mathbf{H}_i/\partial t = -\partial(\nabla \times \mathbf{A})/\partial t, \tag{3}$$

Where $\mathbf{A}$ is the vector potential of the gradient coils.

Similarly, Ampere's law can be written as

$$\nabla \times (\mathbf{H}_i + \mathbf{H}_s) = \sigma(\mathbf{E}_i + \mathbf{E}_s) + \varepsilon_0\varepsilon_r\partial\mathbf{E}/\partial t. \tag{4}$$

Now in the problems at hand,

$$\nabla \times \mathbf{H}_i = \varepsilon_0\partial\mathbf{E}_i/\partial t. \tag{5}$$

So, from Eqs. (4) and (5), one can obtain

$$\varepsilon_0\partial\mathbf{E}_i/\partial t + \nabla \times \mathbf{H}_s = \sigma\mathbf{E}_s + \sigma\mathbf{E}_i + \varepsilon_0\varepsilon_r\partial\mathbf{E}/\partial t. \tag{6}$$

At low frequencies, inside the body, the conduction current is much larger than displacement current, i.e., $\sigma\mathbf{E}_i \gg \varepsilon_0\partial\mathbf{E}_i/\partial t$. Therefore, the component $\varepsilon_0\partial\mathbf{E}_i/\partial t$ can be ignored when considering eddy currents ($\sigma(\mathbf{E}_s + \mathbf{E}_i)$) and the following relationship can be deduced

$$\begin{aligned}\nabla \times \mathbf{H}_s &= \sigma\mathbf{E}_s + \sigma\mathbf{E}_i - \varepsilon_0\partial\mathbf{E}_i/\partial t + \varepsilon_0\varepsilon_r\partial\mathbf{E}/\partial t \\ &\approx \sigma\mathbf{E}_s + \sigma\mathbf{E}_i + \varepsilon_0\varepsilon_r\partial\mathbf{E}/\partial t = \sigma\mathbf{E} + \varepsilon_0\varepsilon_r\partial\mathbf{E}/\partial t.\end{aligned} \tag{7}$$

So, the final formulations can be written as:

$$\begin{aligned}&\begin{cases}\mu\partial\mathbf{H}_S/\partial t = -\nabla \times \mathbf{E} + \mathbf{M}_i \\ \varepsilon_0\varepsilon_r\partial\mathbf{E}/\partial t = \nabla \times \mathbf{H}_S - \sigma\mathbf{E}\end{cases} \quad \text{Inside the body;} \\ &\begin{cases}\mu\partial\mathbf{H}_S/\partial t = -\nabla \times \mathbf{E}_S \\ \varepsilon_0\partial\mathbf{E}_S/\partial t = \nabla \times \mathbf{H}_S\end{cases} \quad \text{Outside the body.}\end{aligned} \tag{8}$$

Table 1
Tissue layers[a] (r: radii (mm)) and the dielectric data[b] ((σ, ε_r): conductivity (S/m), relative permittivity) of the sphere model at 1 kHz

Data	Layer						
	White matter	Gray matter	CSF	Skull	Muscle	Fat	Skin
r	60	80	84	88	92	98	100
σ	0.0626	0.099	2.000	0.0202	0.321	0.0224	0.0002
ε_r	69813	164060	109	2702	434971	24105	1136

[a] [19] and references therein.
[b] Reference: http://www.brooks.af.mil/AFRL/HED/hedr/.

In this way, the scattered component is used for **H** field calculations in all space; while for **E** field calculations, the total field is considered inside the body, but only the scattered field is calculated in free space. The interaction with the gradient coil structure is ignored since it is minimal for gradient fields. The magnetic currents $\mathbf{M}_i$ can be readily calculated using low-frequency electromagnetic formulations [13].

3. Simulations

A previously developed FDTD computer code [10] was modified for the eddy current field calculations. The electromagnetic source, distributed equivalent magnetic currents (DEMC), generated by gradient coils are evaluated using a vector magnetic potential expression [5,13]. In the calculations, the transverse coils are approximated by polygons and the expressions for circular coils such as *z*–coils are computed using elliptic integral expressions. In this study, the coils are driven by sinusoidal varying current of 1 kHz. The gradient coil data is obtained from designs based on a simulated annealing optimization method [14]. Note that only the locations within the biological model require a calculation of the DEMC. Where the design patterns are not known, the gradient magnetic field can be measured, interpolated and used to derive a DEMC. The electromagnetic data of the human body used in this work is obtained from the US Air Force Research Laboratory (http://www.brooks.af.mil/AFRL/HED/hedr/), which represents a large male. The original spatial resolution of the model is 1 mm. For the numerical computation, the model is mapped onto a defined grid with volume-averaged conductive properties. There are a total of 40 segmented tissues in the whole body model. For the FDTD calculation, a three dimensional, 12-layered PML absorbing boundary [10,12], which truncates the computational domain, is deployed around the biological model.

Calculation of the eddy currents in a multilayered sphere model

Before embarking on the body model calculations, it is useful to investigate the eddy currents induced in biologically useful phantoms [15–17]. Here we first consider a head model which is a seven-layered, concentric spherical volume conductor, with similar radial conductivity and permeability profiles as a human head (see Fig. 1A). The layers are structured to attempt to represent a typical head structure. The phantom details are described in Table 1. In this table, the dielectric data is also from the described body model. In the numerical implementation, the cell size is 2 mm. In this case, a typical *z*–Gradient coil (20 loops [14]) was considered.

As the positioning of the subject plays a role in the severity of the response to nerve stimulation, we investigated a series of phantom positions with respect to the gradient coil system (see Fig.1A): from the coil center to the end of the coil windings, where the largest magnetic fields exist. The simulation results are shown in Fig. 1B.

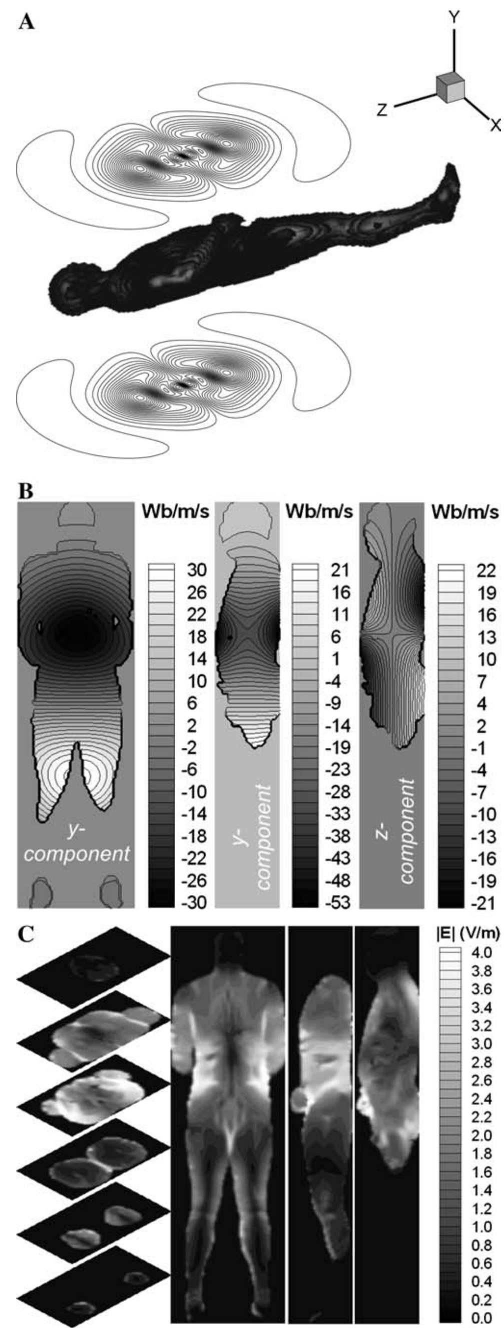

Fig. 2. Calculation of the induced electric fields inside the human whole-body model excited by a typical planar gradient *y*–coil [14]. (A) Schematic arrangement of the human model inside the coils. To generate a slew rate of $dB/dz/dt \approx 100T/m/s$, the coil current is about 300.0 A and the frequency is 1 kHz. (B) The distributed equivalent magnetic current profile (see Eq. (3)). (C) The calculated induced E-field profile.

From this figure, it can be seen that the induced eddy currents were larger near the winding end and lower at the centre, and also the conductivity profile influenced the local field values. In this model, the current density maximum was localized deep within the phantom even though the E-field maximum still occurs at the surface. This type of information cannot be obtained from homogeneous isotropic models. Clearly the induced fields are sensitive to the model parameters. As shown in Fig. 1B, the numerical method is also verified against the available analytic solutions expressed by Debye potentials [1,18]. The comparison demonstrates that both methods generated similar values and the results reflect the effect of inclusion of the highly-contrasted conductivity profiles on the eddy current distribution.

Calculation of the E-fields in a whole-body human model

In this case, we implement a more complicated simulation, a human whole-body model in planar y-Gradient coils, as shown in Fig. 2A. Fig. 2B illustrates the DEMC profile at $y = 0$ plane (left) and $x = 0$ (middle and right) plane, which was employed as an EMF source in the FDTD calculations. As mentioned before, the values used for the electrical properties of [the] human body were obtained from US Air Force Research Lab, and the detailed data at 1 kHz can also be found in [6]. For this calculation, a cell size of 10 mm was used, so the entire computational domain was divided into $N_x \times N_y \times N_z = 103 \times 78 \times 232 \approx 1.8 \times 10^6$ cells. The human body model containing 357,918 cells was placed in the center. The numerical simulation ran for 5000 iterations with a ramp-up peak at 2000 iterations. The total computational time was about 1 h on a DELL computer with single Intel P4 CPU (2.4G Hz).

The result for the E-field distribution is shown in Fig. 2C. From this figure, it can be seen that the induced field pattern is complicated due to the anatomical structure of the body. In general terms, the E-fields are larger away from the centre of the body, as expected, and at the resolution used here, there may be even larger fields just outside the outermost voxels.

For comparison and validation, we have also calculated the E-fields using a previously-published low-frequency FDTD method [10] as a standard. The same gradient coil (see Fig. 2A) was used for both simulations. In the standard FDTD calculation, all the coil wires were discretized into a mesh of Yee cells as current source (see Fig. 3A), and the cell-size was also chosen to be 10 mm. Smaller cell sizes are, of course, possible. Fig. 3C shows the results obtained from the low frequency FDTD scheme. Only the E-fields at $y = 0$ plane have been provided for illustration. From this result and Fig. 2C, it can be seen that similar field patterns were generated. The standard FDTD method, however, required about 4 h to obtain the final solution, which is much longer than the DEMC-based FDTD scheme. A further advantage of the new scheme is that it is able to calculate transient solutions and so the temporal behaviour of induced currents and fields can be studied for any gradient waveform and configuration.

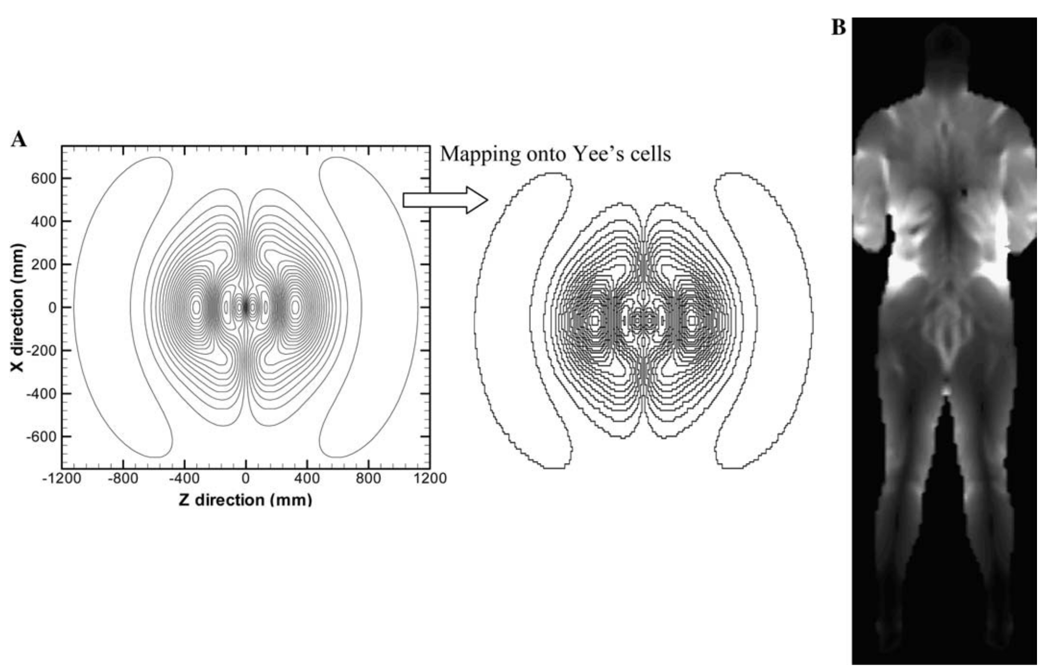

Fig. 3. Calculation of the induced E-fields inside the human whole-body model excited by the same y-Gradient coils as shown in Fig. 2. (A) The illustration of the mapping of the wires onto the staggered Yee cells for standard low-frequency FDTD method; (B) The E-field profile at $y = 0$ plane generated by low-frequency FDTD method (B,[10]) with cell-size of 10 mm. The gray-scale used in this figure is the same as that used in Fig. 2C.

4. Conclusion

A new, modified numerical method for the analysis of gradient-induced effects in the human body has been presented. The method is a variant on the FDTD approach and essentially allows modelling of the interaction of EM fields with tissue where the source has a complex geometric structure. The main advantage of this algorithm is that it does not need to discretize complicated wire structures into a mesh of Yee cells. Furthermore, the computational resources required are reduced since the method only considers the space occupied by the human body.

Acknowledgments

Financial support for this project from the Australian Research Council and NIH (P41 RR16105) is gratefully acknowledged.

References

[1] J.M. Jin, Electromagnetic design and analysis in magnetic resonance imaging, CRC, Boca Raton, FL, 1999, pp. 211–271.
[2] R. Bowtell, R.M. Bowley, Analytic calculations of the E-fields induced by time-varying magnetic fields generated by cylindrical gradient coils, Magn. Reson. Med. 44 (2000) 782–790.
[3] F. Schmitt, K. Stehling, R. Turner (Eds.), Echo-planar imaging theory, technique and application, Springer, Berlin, 1998.
[4] O.P. Gandhi, X.B. Chen, Specific absorption rates and induced current densities for an anatomy-based model of the human for exposure to time-varying magnetic fields of MRI, Magn. Reson. Med. 41 (1999) 816–823.
[5] F. Liu, H.W. Zhao, S. Crozier, On the induced electric field gradients in the human body for magnetic stimulation by gradient coils in MRI, IEEE Trans. Biomed. Eng. 50 (2003) 804–815.
[6] F. Liu, L. Xia, S. Crozier, Influence of magnetically-induced E-fields on cardiac electric activity during MRI: a modelling study, Magn. Reson. Med. 50 (2003) 1180–1188.
[7] C.M. Collins, B.A. Chronik, Modeling human tissues in pulsed gradient fields, Proc. ISMRM (2003) 2440.
[8] G. McKinnon, Simplifying gradient coil modeling in FDTD calculations, Proc. ISMRM (2003) 2437.
[9] G. McKinnon, A quasi-static FDTD approximation reduces computation time, Proc. ISMRM (2003) 2438.
[10] F. Liu, S. Crozier, H.W. Zhao, B. Lawrence, Finite-difference time-domain based studies of MRI pulsed field gradient-induced eddy currents inside the human body, Concept Magn. Reson. 15 (B) (2002) 26–36.
[11] H.W. Zhao, S. Crozier, F. Liu, Finite difference time domain (FDTD) method for modeling the effect of switched gradients on the human body in MRI, Magn. Reson. Med. 48 (2002) 1037–1042.
[12] A. Taflove, Computational Electrodynamics, The Finite-Difference Time-Domain Method, Artech House, Boston, 1995.
[13] D.K. Cheng, Field and Wave Electromagnetics, Addison-Wesley Pub. Co., Reading, Mass, 1989.
[14] S. Crozier, D. Doddrell, Gradient-coil design by simulated annealing, J. Magn. Reson. 103 (A) (1993) 354–357.
[15] M. Bencsik, R. Bowtell, R.M. Bowley, Electric fields induced in a spherical volume conductor by temporally varying magnetic field gradients, Phys. Med. Biol. 47 (2002) 557–576.
[16] M. Bencsik, R. Bowtell, R.M. Bowley, Using the vector potential in evaluating the likelihood of peripheral nerve stimulation due to switched magnetic field gradients, Magn. Reson. Med. 50 (2003) 405–410.
[17] J.R. Keltner, J.W. Carlson, M.S. Roos, S.T.S. Wong, T.L. Wong, T.F. Budinger, Electromagnetic fields of surface coil in vivo NMR at high frequencies, Magn. Reson. Med. 22 (1991) 467–480.
[18] F. Liu, S. Crozier, Electromagnetic fields inside a lossy multilayered spherical head phantom excited by MRI coils: models and methods, Phys. Med. Biol. 49 (2004) 1835–1851.
[19] D.Z. Yao, High-resolution EEG mappings: a spherical harmonic spectra theory and simulation results, Clin. Neurophysiol. 111 (2000) 81–92.